Pergamon

PII: S0038-092X(98)00080-2

Solar Energy Vol. 63, No. 5, pp. 293–302, 1998

0038-092X/98 $—see front matter

ON OPTICAL PERFORMANCE AND DIRECTIONAL CHARACTERISTICS OF PLASTIC FILM LIQUID LAYER SOLAR WATER HEATERS

P. T. TSILINGIRIS†

Technological Educational Institute of Athens, Department of Energy Engineering, A. Spiridonos str., GR122 10, Egalco, Athens, Greece

Received 8 September 1997; revised version accepted 23 June 1998

Communicated by M. G. HUTCHINS

Abstract—An analysis is developed for the investigation of the transmittance–absorptance product ($\tau\alpha$), and directional characteristics of plastic-film water-bag solar water-heaters, which are important for long-term system performance investigations. The analysis allows a complete comparative investigation of the effects of a large number of parameters, like water layer thickness, bottom solar absorptance, radiation transmission conditions and extinction properties of semi-transparent films, on the transmittance–absorptance product. Finally the comparative effect of diffuse and specular reflection and transmission assumption on the derived results is investigated. It is concluded that the use of low iron content glass panes may possibly lead to ($\tau\alpha$) figures far in excess of 0.8 for new systems. © 1998 Elsevier Science Ltd. All rights reserved.

1. INTRODUCTION

Long-term performance of solar energy systems is strongly influenced by the performance of the solar collector subsystem which itself is strongly determined by its optical characteristics. The efficiency of most solar collectors, aiming to trap and convert as much as possible of the incoming solar radiation to heat, depends on the ($\tau\alpha$) and the directional characteristics of the specific glazing system. As far as the glazing systems of ordinary flat plate collectors are concerned, these characteristics can easily be determined either experimentally, by measurements on full size field models, or theoretically, employing ordinary ray tracing techniques. In glazing systems of a more complex configuration, the application of ray tracing procedures over successive multiple parallel semi-transparent regions in contact with materials of different optical characteristics may become very complicated and their effectiveness may become questionable, owing to the increase of the number of possible reflection and refraction paths. This was noticed in the early 1970s by Siegel (1973), who was the first to adapt the application of the net radiation method for enclosures with opaque surfaces to the situation with semi-transparent regions. In this method, a set of $2N$ simultaneous equations is developed for the N interfaces of the glazing system. The equations are solved simultaneously by using conventional numerical procedures for any direction of the incident radiation and, therefore, the method is best suited for computerised solutions. It has been used repeatedly in the literature by many investigators, either to calculate the effect of multi-partially absorbing parallel regions of complex collector glazings Wijeysundera, 1975; Edwards, 1977) or even to investigate the transmission through a random medium of water and glass (Witte and Newell, 1986).

The method can be readily applied to the investigation of ($\tau\alpha$) and directional characteristics of large scale plastic-film water-bag solar collectors. These collectors, proposed recently by Tsilingiris (1997), are an improved design version of the conventional shallow solar pond design, first proposed by Casamajor and Parsons (1979). Investigation of their long-term performance and operational behaviour has shown that they may serve as excellent all-year-round or seasonal water heaters. The significant long-term efficiency along with their simple design, which allows a considerable unit cost reduction, may possibly lead to the development and promotion of large solar heating systems at a competitive price, even at the present time of relatively low-cost conventional energy. Owing to the complete lack of analytical data on ($\tau\alpha$) of the proposed new collector, the previously developed long-term performance

†ISES member.

analysis was based on a reasonable estimate rather than on an accurate analytical calculation of the optical characteristics of the proposed system.

The purpose of the present work is two-fold. Firstly, to apply the net radiation method for the calculation of $(\tau\alpha)$ for normal incidence and angular dependance of the given, rather unusual optical system composed of parallel semi-transparent regions of glass, polymer and water, and secondly, to confirm the $(\tau\alpha)$ assumptions previously made for the long-term performance predictions of the proposed novel solar system design.

2. PHYSICAL PROCESSES AND ASSUMPTIONS

The proposed large area solar collector arrays can easily be installed at any horizontal surface, either roof of building or even on the soil, at a fractional cost as compared with conventional flat plate collectors, using few in situ assembled, standardised factory made modular parts made of recyclable materials, allowing quick erection and upscaling the size of the collector field with a minimum of plumbing.

The design of the modular units as shown in Fig. 1 is based on a large area polymer watertight bag (2), containing a water layer at a fixed thickness. The bag is made by two polymer film layers, a clear one at the top and a dark one underneath, sealed along edges and cut to standardised modular dimensions to fit on an in situ assembled factory-made modular container (1), made of a hard cellular polymer thermal insulation material, sealed at the top with glass panes (3), supported by the edges of the container.

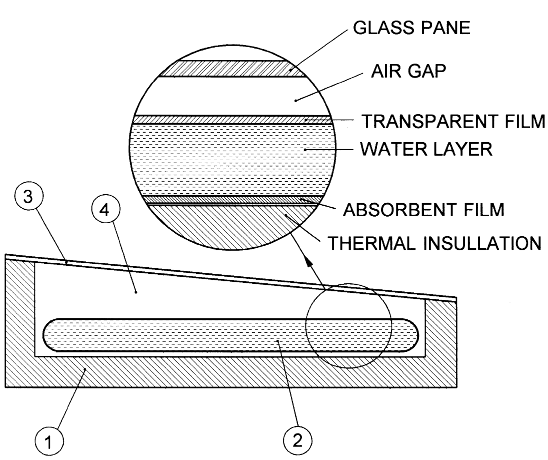

Fig. 1. The basic schematic drawing of the collector with the polymer container (1), water layer bag (2), glazing (3), and air gap between water bag and glazing (4). In the close-up section the water layer is shown contained between the top transparent and lower dark polymer films (not to scale).

The incident solar radiation striking the upper glass surface is partly reflected upwards, with the remainder being refracted and transmitted towards the lower glass–air interfaces. The beam of incoming radiation striking the interface between two semi-transparent materials with different

refractive indices n_1 and n_2 at an incidence angle θ_i undergoes refraction following Snell's law, according to which the angle of refraction is given by,

$$\theta_r = \arc \sin[(n_1/n_2) \cdot \sin \theta_{in}], \qquad (1)$$

and reflection loss by the familiar Fresnells law as the average value of the two components of polarisation of the unpolarised incident beam,

$$r = \frac{1}{2} \cdot [\sin^2(\theta_r - \theta_{in})/\sin^2(\theta_r + \theta_{in}) + \tan^2(\theta_r - \theta_{in})/\tan^2(\theta_r + \theta_{in})]. \qquad (2)$$

The refracted beam is transmitted through the mass of the semi-transparent medium, being further attenuated according to Beer's law,

$$\tau = \exp[-k(d/\cos \theta_r)] \qquad (3)$$

where k is the extinction coefficient of material and $d/\cos \theta_r$ the actual path length of beam.

When incident radiation is diffuse it can be simply treated as a beam with an equivalent angle of incidence at 60°. The phenomenon of dispersion is responsible for the wavelength dependence of the refractive index for most optical materials. Extensive investigations have been carried out for the evaluation of refractive index for water and glass.

Hale and Querry (1973), based on a critical literature review of the existing literature, reported optical constants of water for a wide wavelength range between 0.2 and 200 μm. According to these, the refractive index depends slightly on wavelength, the variation being less than about 1.9% through the wavelength range of interest between about 0.3 and 1.3 μm. There is also a slight temperature dependance of the refractive index of water, which is less than 1% for the temperature range of interest between 15 and 85°C, for a fixed wavelength corresponding to the sodium D line of the spectrum ($\lambda =$

0.58932 μm), according to CRC Handbook of Chemistry and Physics (1983).

Hsieh and Su (1979), have reported the results from extensive investigations on measurements of refractive index of glass in the wavelength range between 0.32 and 206 μm. According to the reported data there is also a slight wavelength dependance for the refractive index of glass, which was found to be less than 2.7% for the wavelength range between 0.32 and 1.3 μm. Therefore, for the purpose of the calculations it was decided to fix the refractive indices of water and glass at the values of 1.329 and 1.526, respectively.

Although the absorption coefficient for glass may be as low as 4 m^{-1} for modern low iron solar collector glass panes, it was taken to be 30 m^{-1} for the purpose of the present analysis, a value which corresponds to ordinary high iron content glass (Dietz, 1954).

According to O'Brien-Berrnini and McGowan (1984), there is a considerable spread of data for the, refractive index and absorption coefficient of various plastics. The refractive index of common polymer materials ranges from values very close to water, like 1.343 for Teflon, up to values as high as 1.64 corresponding to Mylar.

These figures are extremely close to the data reported by Edlin (1981), who also indicate the corresponding ASTM test procedure for the evaluation of refractive index.

Although a closer look on one of those standards with the designation number D542-50 suggests that the results are derived from spectral measurements carried out by an Abbe refractometer illuminated by sodium light, the comparative data, presented by Edlin (1981), indicate a slight wavelength dependance of refractive index which varies smoothly from about 0.3 μm upto near the IR region of the solar spectrum for most plastics of interest. This dependance for teflon and tedlar was found to be less than about 1.5 and 1.4%, respectively, in the wavelength range between 0.4 and 1.4 μm.

The absorption coefficient for various plastics may vary over a considerably wide range between about 9 and 205 m^{-1}, corresponding to acrylics (perspex) and polyesters (Mylar), respectively. For the purpose of the present analysis the values of 1.46 for the refractive index and 140 m^{-1} for the extinction coefficient, close to average for plastics and close to, polyvinyl fluoride were selected.

Although a gradual accumulation of dust and airborn dirt at the topmost air–glass interface probably tends to decrease the proportion of specularly reflected radiation, as a result of the cyclic natural cleaning processes caused by rainfall, the reflection at the topmost glass pane is assumed to be specular. It should be noted here that the idealised assumption of purely specular or purely diffuse reflection or transmission can never be satisfied and both processes are practically partially diffuse and partially specular, depending on the condition and nature of optical surfaces.

Most widely spread practical plastic films appear to have a slightly cloudy or diffusing appearance which favors diffuse transmission. Although many scatter almost uniformly over the solar spectrum, some other may exhibit a wavelength selective behaviour being strongly scattering in the visible, but becoming non-scattering in the near IR, as happens, for example, with teflon which is almost completely non-scattering in the wavelength range between 1 and 2.5 μm. This special selective behaviour for some materials will be neglected for the purpose of the present analysis.

The cloudy appearance of most films is due to the heterogeneous structure of polymer materials with usually coexisting ordered and disordered domains of macromolecules. Their degree of cloudiness depends on the proportion of the crystalline material, usually known as the index of crystallinity. Although this proportion in pure, new polymer film materials can initially be very high, it may be strongly diminished under the effect of the UV radiation of the solar spectrum and the adverse environmental conditions through the process of ageing. In addition to this, the unavoidable gradual deposition of thin airborn dust particles at the surface of the polymer bag due to small amounts of infiltrating air, would gradually shift specular reflection and transmission to diffuse, with a degree proportional to the age of the films.

Solar radiation penetrating the surface of water is strongly attenuated as a result of absorption and scattering in pure water molecules and suspended, dissolved and colloidal matter. Since both phenomena are strongly wavelength dependent, pure water exhibits a strongly wavelength selective behaviour with a transmittance window at the visible range, around 0.48 μm.

Natural waters roughly exhibit a qualitativlely behaviour similar to pure water, with a transparency strongly decreasing with the turbidity level, concentration of suspendent particulate matter, dissolved material and organic pigments, something which usually shifts the maximum transmittance window at longer wavelengths at a degree depending on the origin, nature and concentration of scattering centers.

Owing to the strongly different transmittance behaviour at various regions of the solar spectrum, instead of using a single average value extinction coefficient for the whole solar spectrum, Schmidt (1908) adopted the method of splitting the spectrum into a number of bands (Mullett *et al.*, 1987) attempting to model the transmission of radiation in pure water. Since contemporary data for AM 1.0 solar spectrum and distilled water measurements were used for his calculations, the model was taken to be as an upper bound transmission. This model appeared repeatedly in the oceanographical literature (Defant, 1961) until it was adapted and fitted by Rabl and Nielsen (1975) (R-N), by the sum of four exponential term transmission functions.

The amplitude and exponent of these terms correspond to the energy content and mean extinction coefficient, respectively, over each of the following wavelength bands, 0.2–0.6, 0.6–0.75, 0.75–0.9 and 0.9–1.2 μm, so that derived transmission of the solar spectrum is expressed as the contribution of transmission of each particular band. In solar pond analyses it is always necessary to represent transmission accurately only within the region comprising the gradient zone underneath the upper convecting zone. Therefore, a fifth exponential term corresponding to the IR part of the spectrum (beyond 1.2 μm) is usually completely ignored, since all the energy content of this band is completely absorbed near the top surface and is dissipated mainly through evaporative heat exchange to the environment.

However, for the purpose of the present analysis the radiation transmission model should accurately represent transmission upto the top polymer film and water interface and, therefore, the fifth wavelength band is included, so that transmission is expressed as

$$\tau(x) = \sum_{i=1}^{5} \mu_i \exp(-k_i \cdot x), \qquad (4)$$

with μ_i and k_i properly selected numerical constants (Tsilingiris, 1988).

This simple algebraic model, which is depicted by the solid line in Fig. 2, offers a basic although satisfactory physical interpretation of the attenuation in pure water. More recently, Tsilingiris (1988), recalculated transmission by numerical intergration and by the development of a new 19 exponential term function, using the most recent available data. An appreciably higher upper bound transmission was found as shown by the upper dashed line in Fig. 2, which is attributed to the deficiency of the earlier data and procedures employed by Schmidt.

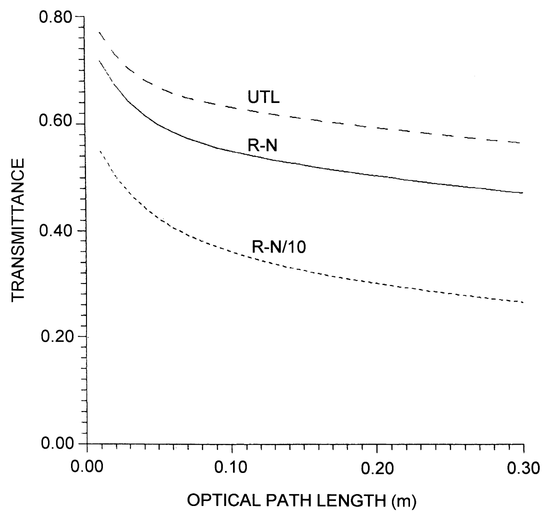

Fig. 2. The models representing the radiation transmission conditions at the water layer. The topmost dashed line and the solid line underneath corresponds to the theoretical upper bound transmission limit and the Rabl–Nielsen transmission models respectively. The lower dashed line represents the turbid layer transmission model.

However, natural waters can never be as clear as distilled water, since even traces of dissolved and suspended matter, colloidal substances and biological growth could be responsible for a strong decrease of spectral extinction coefficients and a dramatic loss of transparency (Enshayan *et al.*, 1988; Tsilingiris, 1991). This effect, although undesirable for salinity gradient solar ponds, would be favorable for the proposed collectors.

Since certain field measurements have shown a remarkably high, close to Rabl–Nielsen transmission, this model is usually arbitrarily accepted to represent transmission, typical for clear natural waters. For the purpose of the present analysis an additional water transmission model was defined to represent data close to typical turbid natural waters. It was found that this model can be fitted, with an adequate accuracy, by an expression similar to eqn (4), with the same amplitudes and an order of magnitude higher exponents, as shown by the lower dotted line of Fig. 2.

The development and growth of biological matter in the stagnant water body of the water bag in indirect systems with an integral copper tube coil heat exchanger, may possibly further increase the proportion of diffuse transmission. Diffuse reflection at the bottom polymer sheet may also be highly likely, as a result of the deposition of silt, foreign matter or mud, especially when using water from groundwater sources.

For the purpose of the present analysis, the reflection and transmission at the air–polymer and polymer–water interfaces, as well as the reflection at the bottom, was assumed to be purely diffuse. This assumption leads to derivation of rather conservative transmittance–absorbance product results at small incidence angles, usually occuring at the periods of the highest solar insolation, since diffuse radiation is treated with an equivalent incidence angle of 60°.

3. MODEL DESCRIPTION AND ANALYSIS

The system model is composed of three semitransparent parallel regions as shown in Fig. 3, with the interfaces between any two media of different refractive indices numbered succesively. The relations between the incoming and outgoing energies at each interface are given by,

$$q_{o,1} = r_g \cdot q_{i,1} + (1 - r_{gd}) \cdot q_{i,2} \quad (5)$$

$$q_{o,2} = r_{gd} \cdot q_{i,2} + (1 - r_g) \cdot q_{i,1} \quad (6)$$

$$q_{o,3} = r_g \cdot q_{i,3} + (1 - r_{gd}) \cdot q_{i,4} \quad (7)$$

$$q_{o,4} = r_{gd} \cdot q_{i,4} + (1 - r_g) \cdot q_{i,3} \quad (8)$$

$$q_{o,5} = r_{pd} \cdot q_{i,5} + (1 - r_{pd}) \cdot q_{i,6} \quad (9)$$

$$q_{o,6} = r_{pd} \cdot q_{i,6} + (1 - r_{pd}) \cdot q_{i,5} \quad (10)$$

$$q_{o,7} = r_{wd} \cdot q_{i,7} + (1 - r_{wd}) \cdot q_{i,8} \quad (11)$$

$$q_{o,8} = r_{wd} \cdot q_{i,8} + (1 - r_{wd}) \cdot q_{i,7} \quad (12)$$

$$q_{o,9} = (1 - a_d) \cdot q_{i,9} \quad (13)$$

$$q_{o,10} = a_d \cdot q_{i,9} \quad (14)$$

The interrelationships between incoming and ougoing radiation quantities are given by the following expressions,

$$q_{i,1} = Q \quad (15)$$

$$q_{i,2} = \tau_{gd} \cdot q_{o,3} \quad (16)$$

$$q_{i,3} = \tau_g \cdot q_{o,2} \quad (17)$$

$$q_{o,4} = q_{i,5} \quad (18)$$

$$q_{i,4} = q_{o,5} \quad (19)$$

$$q_{i,7} = \tau_{pd} \cdot q_{o,6} \quad (20)$$

$$q_{i,6} = \tau_{pd} \cdot q_{o,7} \quad (21)$$

$$q_{i,8} = \tau_{wd} \cdot q_{o,9} \quad (22)$$

$$q_{i,9} = \tau_{wd} \cdot q_{o,8} \quad (23)$$

$$q_{i,10} = 0 \quad (24)$$

By substitution of eqns (11)–(20) into eqns (1)–(10) and dividing by Q, the following relationships are derived,

$$-(q_{o,1}/Q) + (1 - r_{gd}) \cdot \tau_{gd} \cdot (q_{o,3}/Q) = -r \quad (25)$$

$$-(q_{o,2}/Q) + r_{gd} \cdot \tau_{gd} \cdot (q_{o,3}/Q) = -(1 - r_g) \quad (26)$$

$$-(q_{o,3}/Q) + r_g \cdot \tau_g \cdot (q_{o,2}/Q) + (1 - r_{gd}) \cdot (q_{o,5}/Q) = 0 \quad (27)$$

$$-(q_{o,4}/Q) + r_{gd} \cdot (q_{o,5}/Q) + (1 - r_g) \cdot \tau_g \cdot (q_{o,2}/Q) = 0 \quad (28)$$

$$-(q_{o,5}/Q) + r_{pd} \cdot (q_{o,4}/Q) + (1 - r_{pd}) \cdot \tau_{pd} \cdot (q_{o,7}/Q) = 0 \quad (29)$$

$$-(q_{o,6}/Q) + r_{pd} \cdot \tau_{pd} \cdot (q_{o,7}/Q) + (1 - r_{pd}) \cdot (q_{o,4}/Q) = 0 \quad (30)$$

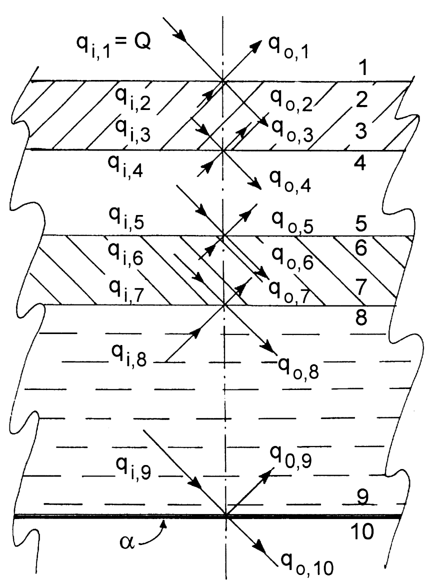

Fig. 3. The theoretical model with the three parallel regions of semitransparent materials and the ten interfaces. The glass pane at the top and the plastic film underneath the air gap with the fluid layer sitting on the bottom absorbing film with an absorptivity α (the parallel regions shown are not to scale).

$$-(q_{o,7}/Q)+r_{wd}\cdot\tau_{wd}\cdot(q_{o,9}/Q)+(1-r_{wd})\cdot\tau_{wd}\cdot(q_{o,9}/Q)=0 \quad (31)$$

$$-(q_{o,8}/Q)+r_{wd}\cdot\tau_{wd}\cdot(q_{o,9}/Q)+(1-r_{wd})\cdot t_{pd}\cdot(q_{o,6}/Q)=0 \quad (32)$$

$$-(q_{o,9}/Q)+(1-a_d)\cdot\tau_{wd}\cdot(q_{o,8}/Q)=0 \quad (33)$$

$$-(q_{o,10}/Q)+a_d\cdot\tau_{wd}\cdot(q_{o,8}/Q)=0. \quad (34)$$

A flexible numerical code was developed for the numerical solution of the system of eqns (25)–(34), using the Gauss elimination method. The system of eqns (21)–(30) was translated to its matrix form by

$$\mathbf{A}.X=\mathbf{B}, \quad (35)$$

with X the solution array and **A** and **B** a rectangular 10×10 matrix and a one-dimensional array, respectively, the elements of which were introduced for the repetitive calculations in the code. The interactive, user friendly computer code solves the equations, which are carried out in the region of the incidence angles between 0 and 90° with a 3° step, allowing wide-range parametric investigations through the direct selection and interchange of a large number or group parameters. The derived results are employed for the validation of the radiative balance at each parallel interface of the optical system for any angle step at the entire defined domain of incident angles.

4. RESULTS AND DISCUSSION

Derived results were plotted in the form of $(\tau\alpha)$ figures against the incidence angle of the incoming radiation, ranging between 0 and 90° at a uniform coordinate system, allowing direct comparisons of the relative effects between various design parameters.

The results were derived under the assumption of an extinction coefficient for glass and plastic equal to 30 and 140 m^{-1}, respectively. The thickness of glass pane and plastic foil was taken to be 4 and 0.3 mm, respectively, which corresponds to a kd product equal to 0.12 and 0.042, respectively.

The effect of water layer thickness in the $(\tau\alpha)$ is shown in Fig. 4, with the water layer thickness of 0.025, 0.05, 0.1 and 0.2 m as a parameter for a typical system with a bottom solar absorptance fixed at 0.9 and radiation transmission following the R-N model.

It is shown that under the assumption of diffuse transmission and reflection, and using the selected conservative figures of low optical grade materials, results very close to 0.7 were obtained. It can also be seen that the $(\tau\alpha)$ is proportional to the water layer thickness. However, the effect of the deepest layers even at the longest path lengths, being less than 3% at near normal incidence is rather insignificant.

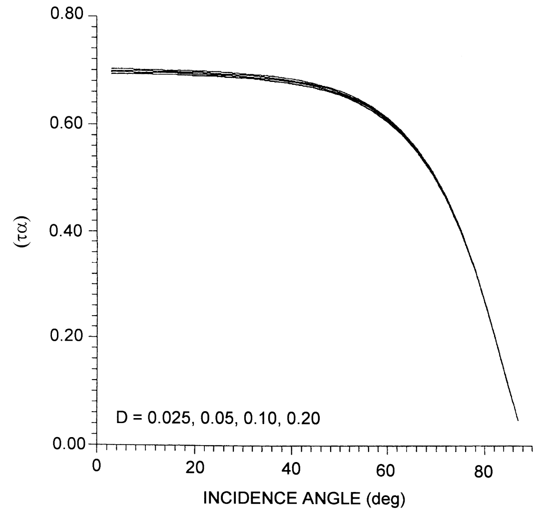

Fig. 4. The angular dependence of transmittance–absorptance product as a function of the water layer thickness for a bottom absorptivity fixed at 0.9. The topmost of the four lines corresponds to $D=0.2$ m while the lower line to $D=0.025$ m.

This is attributed to the small effect of the water layer thickness on the absorption of the bottom reflected radiation, which for $\alpha=0.9$ is a small fraction of the incident solar radiation anyway. The effect of water layer thickness is expected to become more significant as the bottom absorptance decreases. This leads to a growing fraction of upwards reflected radiation and absorption of the outgoing radiation at a rate proportional to the water layer thickness.

The effect of bottom solar absorptance in $(\tau\alpha)$ is shown in Fig. 5, in which the plotted results are groups of fixed bottom absorptance lines corresponding to $\alpha=1$, 0.8 and 0.6. According to the derived results based on the R-N transmission model, the effect of the variation of the water layer thickness between 0.025 and 0.2 m on $(\tau\alpha)$, ranges for near normal incidence between about 6, 3 and 0% for a bottom absorptance of 0.6, 0.8 and 1.0, respectively. There is completely no effect of water layer thickness on $(\tau\alpha)$, as shown by the coincidence of the upper group of broken lines correspond-

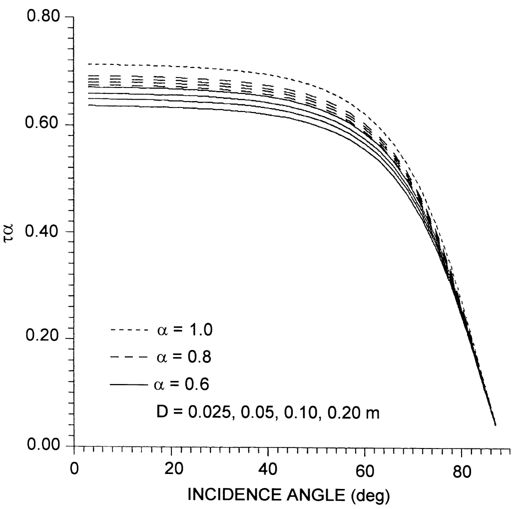

Fig. 5. The angular dependance of transmittance–absorptance product as a function of bottom absorptivity. The three groups of four lines correspond to $\alpha = 1.0$ (topmost identical dashed lines), $\alpha = 0.8$ (lower group of dashed lines) and $\alpha = 0.6$ (lower group of solid lines). The topmost and the lower three lines in each group of four correspond to $D = 0.2$, 0.1, 0.05 and 0.025 m, respectively.

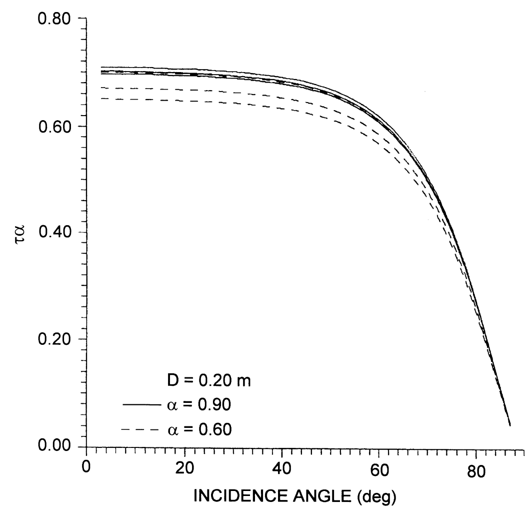

Fig. 6. The effect of radiation transmission conditions on the angular dependance of transmittance–absorptance product. The upper group of three solid lines correspond to $\alpha = 0.9$ while the lower group of three dashed lines to $\alpha = 0.6$. The topmost of the three lines in each group correspond to turbid water transmission model while the lower two to the Rabl–Nielsen's and upper transmission limit, respectively.

ing to bottom absorptance of 1.0, which leads to a near normal $(\tau\alpha)$ figure of about 0.72.

It is therefore confirmed that the growing significance of water layer thickness on $(\tau\alpha)$ at the lower bottom solar absorptance figures, is attributed to the longer path length on the water layer, which leads to a corresponding stronger absorption of the bottom reflected radiation.

A qualitatively similar behaviour is expected for the effect of the rate of extinction of radiation in the water layer on $(\tau\alpha)$. For a fixed layer thickness, a turbid water layer is expected to trap a higher fraction of the upwards reflected radiation than an optically pure layer. Corresponding results are displayed in Fig. 6, derived for a fixed layer thickness of 0.2 m, in which two groups of three lines are shown. The upper group of solid lines correspond to a bottom absorptance of 0.9 while the lower group of dashed lines to 0.6. The topmost of the three lines in each group corresponds to the turbid layer model as defined in clause 2 and shown by the lower dashed line in Fig. 2, while the next lower two, to the R-N and the upper transmission limit models as shown by the solid intermediate and topmost dashed lines in Fig. 2, respectively.

It is shown that although for the investigated range of radiation transmission conditions as shown by the three plotted models in Fig. 2, a bottom absorptance as low as 0.6 leads to a significant effect on near normal incidence $(\tau\alpha)$ of about 7.5%, whereas an increased absorptance of 0.9 leads to a significantly decreased range of about 2%.

For the investigation of the relative effects of extinction of radiation in glass and polymer, similar calculations were carried out and plotted using the same coordinate system for a wide range of the *kd* product. Since the previously employed *kd* value for polymer was 0.042, the calculations were extended for a *kd* parameter ranging more than an order of magnitude between $0.01 \leq (kd)_p \leq 0.11$. For the extinction coefficient of a wide range of plastics, this range may cover most film thicknesses of practical significance. The results are shown in Fig. 7 in which the $(\tau\alpha)$ was plotted against different values of the $(kd)_p$ product of 0.01, 0.06 and 0.11 for a fixed water layer thickness of 0.1 m. The two groups of solid and dashed lines correspond to $\alpha = 1.0$ and $\alpha = 0.8$, respectively, while transmission is assumed to be represented by the R-N model.

It is shown that $(\tau\alpha)$ increases proportionally to $(kd)_p$ at a degree which is proportional to α. This is attributed to the fact that since the plastic film is in contact with the water, the absorbed radiation at the film is considered to be an energy gain for the system which is transferred into the water layer. As the bottom absorptance decreases, the contribution of the

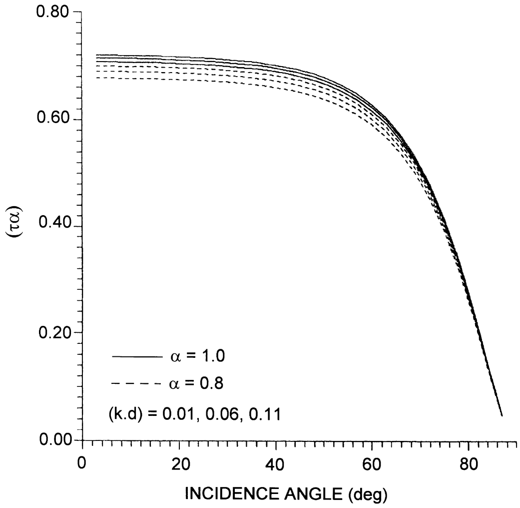

Fig. 7. The effect of the *kd* product for the polymer film on the angular dependance of transmittance–absorptance product for a $D=0.1$ m and Rabl–Nielsen's radiation transmission conditions. The upper group of three solid and the lower group of three dashed lines correspond to $\alpha=1.0$ and $\alpha=0.8$, respectively. The topmost of each group of three lines correspond to $kd=0.11$ while the lower two lines of each groups to 0.06 and 0.01, respectively.

plastic film on the overall energy gain becomes more significant as it is comparatively shown from the effect of variation of $(kd)_p$ on the $(\tau\alpha)$ for $\alpha=0.8$ and 1.0.

The effect of the *kd* product for glass, varying in the range of $0.01 \leq (kd)_g \leq 0.24$ is also shown

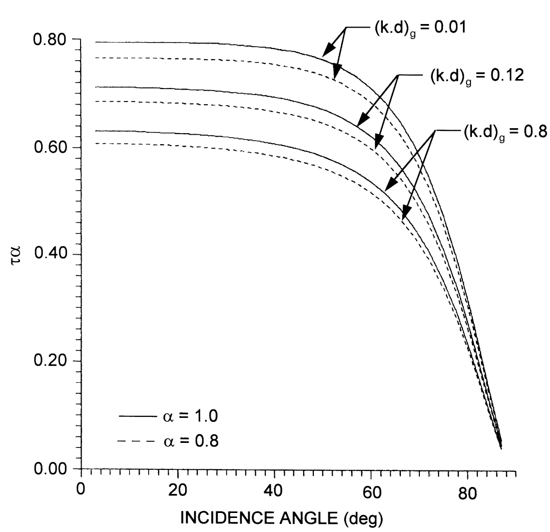

Fig. 8. The effect of *kd* product for the glass pane on the angular dependance of transmittance–absorptance product for $D=0.1$ m and Rabl–Nielsen's radiation transmission conditions. The upper group of three solid lines correspond to $a=1$ while the lower group of three dashed lines to $\alpha=0.8$. The topmost line of each group corresponds to $kd=0.01$ while the lower two correspond to 0.12 and 0.24, respectively.

in Fig. 8 for a fixed water layer thickness of 0.1 m, R-N transmission and $\alpha=0.8$ and 1.0. Taking into account the possible range of extinction coefficients for glass, the selected range of the $(kd)_g$ parameter corresponds to most glass pane thicknesses of practical importance, since its lowest value corresponds to about 3 mm water clear glass while its highest to a 8 mm high iron content glass pane.

It is important that in contrast to Fig. 7, the increase of $(kd)_g$ parameter leads to a corresponding decrease in $(\tau\alpha)$, something which is attributed to the fact that any energy loss at the glass is not directly transferred into water layer, as happens with the polymer bag, and this explains the equal spacing between dashed and solid lines corresponding to $\alpha=0.8$ and 1.0, respectively. It could also be noted here that although the investigated *kd* parameter range for glass is twice that for the polymer, its relative effect is stronger and the use of low iron glass and a bottom polymer film of a high solar absorptance may lead to a $(\tau\alpha)$ figure of 0.8.

The results presented so far, are all based on the assumption of completely diffuse reflection and transmission at all optical interfaces except the outer glass pane. This assumption which can never be completely satisfied in practice, is expected to lead, especially for incident angles less than 60°, to conservative $(\tau\alpha)$ predictions. The derivation of a similar group of results under the assumption of purely specular processes would be very important since they would allow the evaluation of the maximum range within which real data should possibly be expected in practice.

The results of calculations which were based on the angular dependance of reflection and transmission losses at the paralel layers and interfaces were comparatively plotted in Fig. 9 for a fixed water layer thickness of 0.1 m.

Both solid and dashed lines refer to specular and diffuse processes, respectively, with the higher corresponding to $\alpha=1.0$ and the lower to $\alpha=0.8$. It can be seen that the specular assumption although not realistic, especially for old, long-exposed glazing systems with relatively aged polymer films, leads to a $(\tau\alpha)$ as high as 0.8 or even higher when using low iron glass panes, something which confirms the assumption made in earlier long-term performance prediction investigations. These data are appreciably higher than those derived under the assumption of diffuse processes, which although

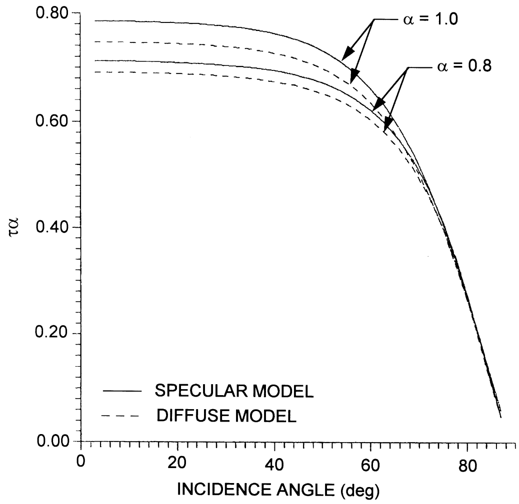

Fig. 9. The effect of specular or diffuse reflection and transmission assumption on the angular dependance of transmittance–absorptance product for Rabl–Nielsen's transmission conditions and $D=0.1$ m. The pair of solid and dashed lines correspond to specular and diffuse processes, respectively. The upper line corresponds to $\alpha=1.0$ and the lower to $\alpha=0.8$.

conservative, maybe proved to lead to unrealistically low results for new systems.

5. CONCLUSIONS

An analysis was developed for the evaluation of the $(\tau\alpha)$ and the investigation of the directional characteristics of plastic film water bag solar collectors. Apart from a few incomplete field measurements carried out on a similar collector design, known as shallow solar ponds (Clark and Dickinson, 1980), there was a lack of such data which are very important for long-term system performance predictions.

As a result of the difficulties involved with the application of conventional ray tracing procedures, the net radiation method was applied for the evaluation of the optical performance and angular dependance of the present relatively complex glazing system. A parametric analysis, which was carried out for a wide range of main design parameters, material characteristics and transmission properties, has allowed the comparative evaluation of their effects on the $(\tau\alpha)$. An effort has also been made to assess the implication of the main assumptions on the derived results, according to which considerably high results can be derived for new glazing systems using low iron glass panes although unavoidable ageing could appreciably degrade the optical performance of the proposed systems.

NOMENCLATURE

A	Rectangular 10×10 matrix
B	One-dimensional array
d	Material thickness (m)
D	water layer thickness (m)
k	Extinction coefficient (m^{-1})
n	Refractive index
q	Radiant energy rate ($w\,m^{-2}$)
r	Reflection loss coefficient
x	Vertical distance (m)
X	Solution array

Subscripts

d	Diffuse
g	Glass
gd	Glass diffuse
in	Incident
i,j	Incoming at the interface j
o,j	Outgoing from the interface j
pd	Polymer diffuse
r	Refracted
wd	Water diffuse

Greek letters

α	Solar absorptance
θ	Angle (°)
μ	Numerical constant (amplitude)
τ	Transmittance
$(\tau\alpha)$	Transmittance–absorptance product

REFERENCES

Casamajor A. B. and Parsons R. E. (1979) Design Guide for Shallow Solar Ponds. Lawrence Livermore Laboratory Report UCRL52385, Rev. 1. to U.S. Dept of Energy.

Clark A. P. and Dickinson W. C. (1980) Shallow solar ponds. In *Solar Energy Technology Handbook*, Part A, ed. W. C. Dickinson and P. N. Cheremisinoff. Marcel Decker, New York, pp. 377–402.

CRC Handbook of Chemistry and Physics (1983) 63th edn, CRC Press, Boca Raton, FL.

Defant A. (1961) *Physical Oceanography*, Vol.1, Pergamon Press, Oxford.

Dietz A. G. H. (1954) Diathermous materials and properties of surfaces. In *Space Heating with Solar Energy*, ed. R. W. Hamilton. MIT Press, Cambridge, MA.

Edlin F. (1981) Optical properties of materials used in solar energy systems. In *Solar Energy Handbook*, ed. J. F. Kreider and F. Kreith. McGraw-Hill, New York, pp. 5-15 to 5-17.

Edwards D. K. (1977) Solar absorption by each element in an absorber–coverglass array. *Solar Energy* **19,** 401–402.

Enshayan K., Golding P., Nielsen C. and Short T. (1988) Solar-radiation attenuation in solar ponds. In *Proc. Int. Solar Pond Progress Conf.*, Cuernavaca Mexico, ed. J. Huacuz, M. Dominiguez and H. Beccera, pp. 66–73. IIE, Cuennaraca.

Hale G. M. and Querry M. R. (1973) Optical constants of water in the 200 nm to 200 μm wavelength region. *Applied Optics* **12,** 3, 555–563.

Hsieh C. K. and Su K. C. (1979) Thermal properties of glass from 0.32 to 206 μm. *Solar Energy* **22,** 37–43.

Mullett L. B., Afeef M. A. and Tsilingiris P. T. (1987) Salt gradient solar ponds a reassessment of efficiency and stability. In *Proc. 5th Int. IEE Conf. Energy Options — The Role of Alternatives in the World Energy Scene*, Reading, U.K., Conf. Publ 276, pp. 78–92. IEEE, London.

O'Brien-Berrnini F. C. and McGowan J. G. (1984) Performance modelling of non-metallic flat plate solar collectors. *Solar Energy* **33,** 3/4, 305–319.

Rabl A. and Nielsen C. E. (1975) Solar ponds for space heating. *Solar Energy* **17,** 1, 1–12.

Schmidt W. (1908) Absorption der Sonenstrahlung in Wasser Sitzungsberichte der Mathematisch-Naturwissenshaftlichen Klasse der Akademie der Wissenshaften, band CXVII, heft I-X, Wien, pp. 237–253.

Siegel R. (1973) Net radiation method for transmission through partially transparent plates. *Solar Energy* **15,** 273–276.

Tsilingiris P. T. (1988) An accurate upper estimate for the transmission of solar radiation in salt gradient ponds. *Solar Energy* **40,** 1, 41–48.

Tsilingiris P. T. (1991) Salinity gradient. *Energy Convers. Mgmt* **32,** 4, 333–343.

Tsilingiris P. T. (1997) Design, analysis and performance of low-cost plastic film large solar water heating systems. *Solar Energy* **60,** 5, 245–256.

Wijeysundera N. E. (1975) A net radiation method for the transmittance and absorptivity of a series of parallel regions. *Solar Energy* **17,** 75–77.

Witte M. J. and Newell T. A. (1986) Transmission of solar radiation through a random medium of water and glass. *Journal of Sol. En. Engineering* **108,** 199–205.